Window Related Thermal Bridges

Benjamin Barnes
Member ASHRAE

Axy Pagán-Vázquez
Member ASHRAE

Richard Liesen, PhD
Member ASHRAE

Justine Yu

Nicholas Alexander

ABSTRACT

Window thermal performance in the US is rated by the National Fenestration Rating Council's (NFRC) Standard 100, which requires estimates of a window frame's effective conductivity. Meanwhile, most energy estimation methods require effective conductivities to be derived for the rest of the wall. These two U-factors, when weighted by their respective areas, however, do not capture the thermal bridging caused by a window installation; flashing, lintels, masonry sills, additional structural framing, and the window frame's interaction with these components can all contribute to thermal bridging. The magnitude of this additional "as installed" thermal bridge is estimated as the difference between area weighted U –factors and a 2D or 3D simulation capturing "as installed" details. Some thermal bridge catalogs now report such values. These "Ψ -values," however, could be different for different windows installed with the same sill detail. This work estimates the sensitivity of a sill detail's "as installed" Ψ -value to the properties of the window frame installed. Six different window frames with progressively lower frame U-factors, from high performance wood to low performance aluminum, are simulated as they would be installed in two common commercial wall constructions with two sill detail strategies. Simulations use the finite-element heat transfer software THERM. Resulting knowledge of the impact of frame characteristics on the Ψ -value suggests that it is not always possible to use the Ψ -value from a catalog if a different window is chosen than that used for the original calculation, especially when combining well-detailed sills with lower performing windows.

BACKGROUND

ISO Standard 10211 defines a thermal bridge as "part of the building envelope where the otherwise uniform thermal resistance is significantly changed by full or partial penetration of the building envelope by materials with a different thermal conductivity, and/or a change in thickness of the fabric, and/or a difference between internal and external areas, such as occur at wall/floor/ceiling junctions" (2007). The calculation method used to determine the increase in thermal transmittance attributable to a thermal bridge is dependent upon the type of bridge encountered. For repeating thermal bridges, like studs or brick ties, the additional heat flow is taken into account in the calculation of the U-values of the surfaces containing the thermal bridges.

For non-repeating thermal bridges, which encompass the window-related bridges discussed in this paper, the heat flow attributable to the thermal bridge is calculated and added separately. For reasons described in Morrison Hershfield (2011), the additional heat transfer should be quantified as the linear thermal transmittance or Ψ -value. The Ψ -value has units of W/(m·K) and expresses the additional heat transfer caused by a feature per unit of length per degree of temperature difference at steady or quasi-steady state.

Window related thermal bridges are particularly interesting because they exhibit all three conditions described in the definition: materials of different resistance, change in the thickness of the building fabric, and a difference between internal and external surface areas. They also occur where the uniform thermal resistance —the building clear wall—meets

***Benjamin Barnes**, **Axy Pagán-Vázquez**, **Richard Liesen**, and **Justine Yu** are researchers at US Army Corps of Engineers, Engineer Research and Development Center, Construction Engineering Research Laboratory, Champaign, IL. **Nicholas Alexander** is a construction representative for US Army Corps of Engineers, USAF Academy, CO.*

Published by ASHRAE 2013

an entirely different type of surface—the window—which is quantified in the US using the area-weighted approach according to NFRC Standard 100 (NFRC 2010). The building clear wall, if determined correctly, captures 2D effects such as repeating structural elements. If the correct component U-factors are used with the correct areas, the window U-factor will capture the 2D thermal effects within the window itself. Estimating a whole wall performance by area-weighting these two resulting U-factors, however, fails to capture the substantial thermal impacts of masonry sills and lintels, flashing, other structural elements related to window installation, and the interaction of these features with the window frame itself.

This window-related thermal bridge is shown for a sill detail as the red shaded area in Figure 1. Figure 1 (b) shows a badly bridged detail and a correspondingly greater red area, while (c) shows a detail that maintains the thermal control layer and has a correspondingly smaller red area. This net additional heat flux, normalized to the temperature difference and the length of the detail, becomes the Ψ-value and can be used as a correction to the assumption pictured in Figure 1(a). The aim of this work is to determine whether this Ψ-value is sensitive to the window chosen, or if it can be considered a property of the sill detail.

Window Thermal Bridge Issues

Schild and Blom (2010) reviewed and compiled the experiences of several European Union (EU) member states' attempts to provide guidance on thermal bridges. Their conclusion was that thermal bridge regulation and guidance should be accomplished via catalogs of recommended details, complete with quantified linear thermal transmittance values. It is also useful to have poorly performing details quantified to facilitate justifying changes or retrofits. Such catalogs free designers from the time consuming and difficult process of performing their own 2D heat transfer simulations for every detail. For windows it is conceivable that a reasonable number of sill, jamb and head details could be quantified and could represent most situations. The catalog detail could even include a specific window position in the wall, which has a well established effect on the Ψ-value, as discussed in Cappelletti et al (2011). If, however, the Ψ-value of the sill, jamb, and head bridges depend strongly on the window frame cross-section interacting with them, beyond simply the frame's position in the wall, the number of required detail permutations expands greatly, and the feasibility of a go-to catalog is decreased. This work aims to explore when it is necessary to compute the Ψ-value of a unique combination of window cross section and installation detail and when it can be taken as independent of the window frame installed and used

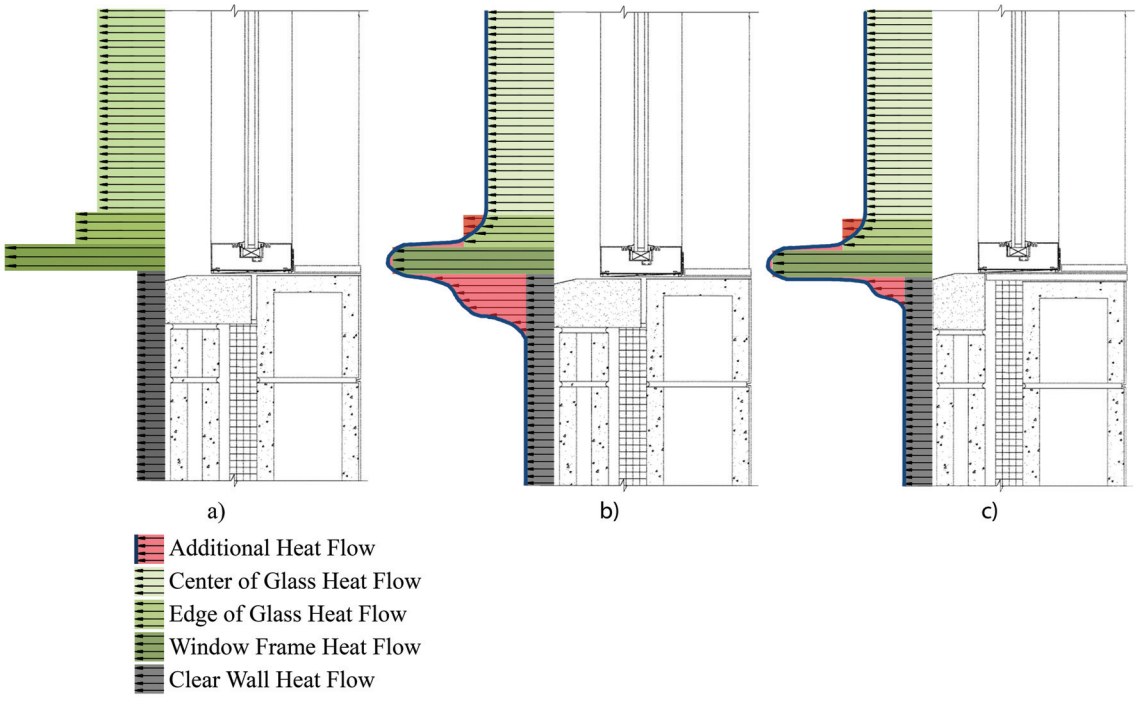

Figure 1 *(a) A common model for estimating whole wall U-factor is to area weight the 1D effects over the window center, edge of glass, frame, and the clear wall. (b) The real heat transfer, shown by the blue line, of a thermally bridged detail. (c) The real heat transfer, shown by the blue line, of an unbridged window detail. Typically, the three window U-factors would be area averaged and modeled as one, uniform U-factor prior to area-weighting with the wall, but they are shown separately here for clarity.*

as a widely applicable catalog detail. Similarly, this will clarify applicability of existing catalogs where the user wishes to specify a different window than the one shown in the catalog detail.

To accomplish this, we will combine multiple wall types and window types across the spectrum of construction techniques and window frame thermal performance. Window sills are used for this work because the window-wall coupling characteristics are thought to be representative for other details; that is, the implications concerning the design of a Ψ-value catalog are expected to be relevant to jamb and head details as well.

Ψ-VALUE CALCULATIONS FOR WINDOWS

Most energy estimation methods require a whole wall U-factor estimated by area-weighting the window U-factor and the clear-wall U-factor. This area-weighting approximates conduction as 1D over each area and implicitly assumes that the two elements meet at an adiabatic plane. These two terms alone fail to capture the thermal impacts of masonry sills and lintels, other structural elements, and the 2D interaction of these features with the window frame itself. A third term, the Ψ-value, makes up for this deficiency and is calculated as the difference between a calculation that includes these complexities and a simple area-weighted approach. For a given wall cross section, these three terms can be expressed as the heat transfer per length of the wall, or thermal coupling coefficient, as in ISO (2007):

$$L_{2D} = U_{\text{clear-wall}} h_{\text{clear-wall}} + U_{\text{window}} h_{\text{window}} + \Psi_{\text{sill}} \quad (1)$$

where:

L_{2D} = thermal coupling coefficient of wall cross section in W/(m·K)

$U_{\text{clear-wall}}$ = U-factor of the wall where no thermal bridges occur in W/(m^2·K)

$h_{\text{clear-wall}}$ = height of clear wall in section

U_{window} = U-factor of the window, typically from area-weighting U-factors from 2D simulations of the frame, edge-of-glass, and center-of-glass regions in W/(m^2·K) (Btu/h·sf·°F)

h_{window} = height of window included in section

Ψ = linear thermal transmittance of a bridge in W/(m·K)

Equation 1 (and this paper) only examines a section containing the sill. To include the full effect on the wall, one would need to include the bridges associated with the jambs and head as well. As discussed above, this paper focuses on sills in order to explore in greater depth the effects of window choice on window-related Ψ-value. The sill thermal bridge heat flow can be calculated by 1) simulating the window frame including 150 mm of glass, following NFRC 100 guidelines, to obtain U_{window}, 2) simulating the clear wall, not including any sill details such as masonry sills and flashing, to obtain $U_{\text{clear-wall}}$, 3) simulating the assembly including all sill details and the window to obtain the thermal coupling coefficient, L_{2D}, and finally 4) solving Equation 1 for Ψ_{sill}.

ASSEMBLIES SIMULATED

Two wall types common to commercial construction were chosen for investigation, including block construction with brick veneer and light gage steel construction with a brick veneer. Both wall types were simulated with high performing (unbridged) and typical (bridged) details. The four resulting combinations are shown in Figures 1 and 2. The bridged details are taken from recent construction documents. To create the unbridged details, the two bridged details are modified to better maintain the thermal control layer as recommended in Lstiburek (2011). The four details are later combined with each of six windows. These windows, shown in Figure 3, represent the performance range of modern window frames, from a very high performance wood window to a typical aluminum curtain wall with a minimal thermal break. All windows were inspired by commercially available windows but are not identical to the actual products. Weep holes, curtain wall bolts, and other fasteners are ignored.

SIMULATION METHODS

THERM 6.3 is used to perform all heat transfer simulations (Finlayson et al. 1998). WINDOW 6.3 is used to create the glazing units and estimate their center-of-glass properties before importing into THERM (Mitchell et al. 2001). Unless otherwise stated, simulations were carried out in accordance with NFRC 100 guidelines, including boundary conditions (NFRC 2010). Though boundary conditions from ISO Standard 6946 (2007) are a more typical choice, this work attempts to discover any relationship between the window and the window-related Ψ-value, and since the window U-factor would normally come from NFRC 100 certification, the wall boundary conditions were taken from this standard to keep from having adjacent boundary conditions differ.

For light gage steel stud walls, the effective conductivity of the stud cavity was determined from a simulation of a plan-view cross section, which accounts for the effect of the vertical studs. The horizontal sill stud is the only steel stud that is explicitly modeled in the section view. The boundary conditions for all simulations were as follows:

1. Internal, non-glazing surfaces were assigned appropriate emissivities based on their materials and were modeled as radiatively communicating with a 21.0°C (69.8°F) room surface and with each other. Where the material was likely to have a higher internal surface temperature (e.g., in the case of the interior wall surface or the interior of a wood window), it was assigned a convection coefficient of 2.44 W/(m^2·K) (0.430 Btu/h·ft^2·°F). In the case of the Aluminum window, where a colder surface is expected, 3.0 W/(m^2·K) (0.528 Btu/h·ft^2·°F) is assigned. Air temperature is 21.0°C (69.8°F).

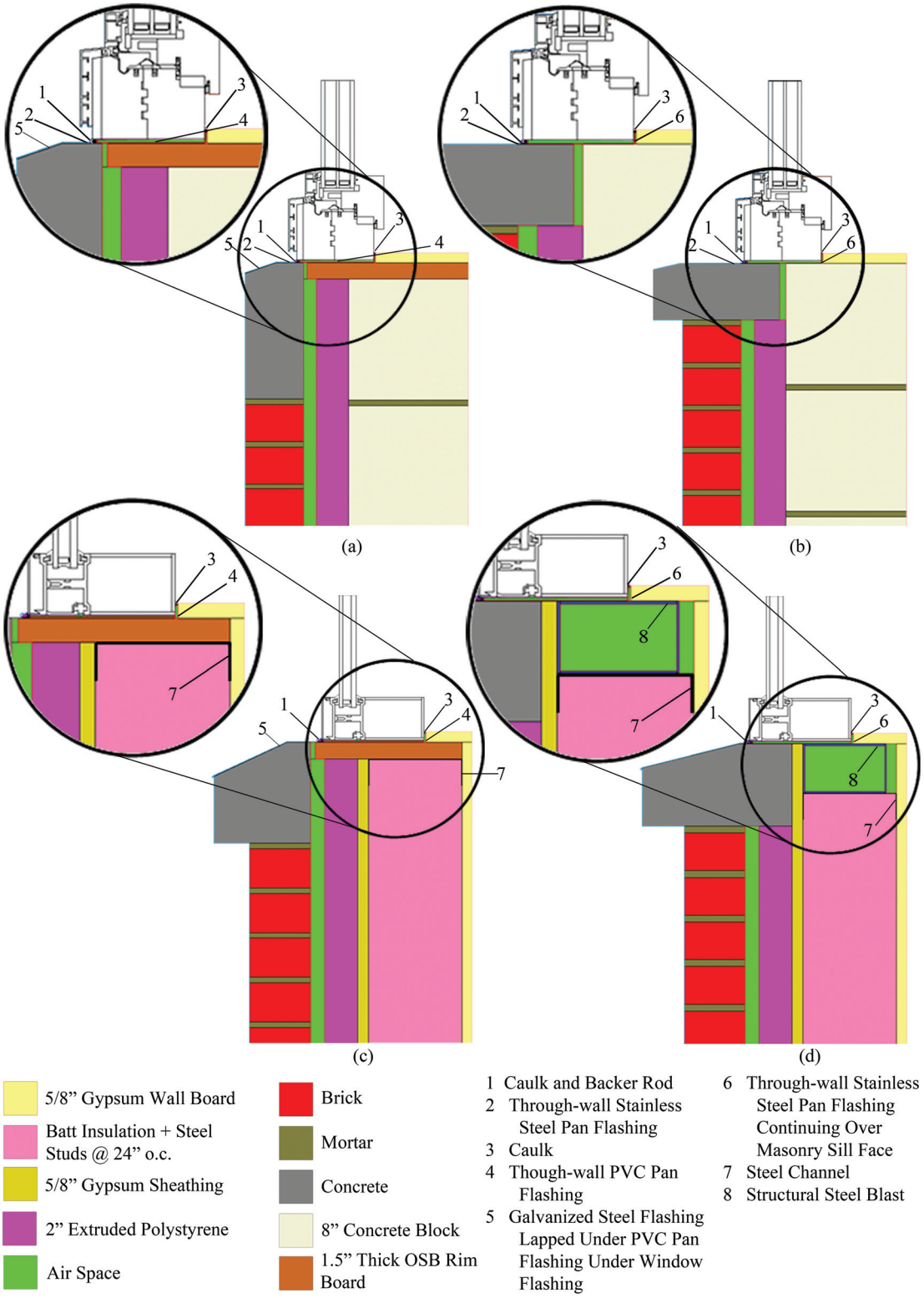

Figure 2 *The four details, made up of two wall types each with bridged and unbridged sills: a) unbridged CMU wall; b) bridged CMU wall; c) unbridged steel stud wall; d) bridged steel stud wall. Note that the four details shown here were studied with all windows, for a total of 24 combinations, not just the four combinations shown.*

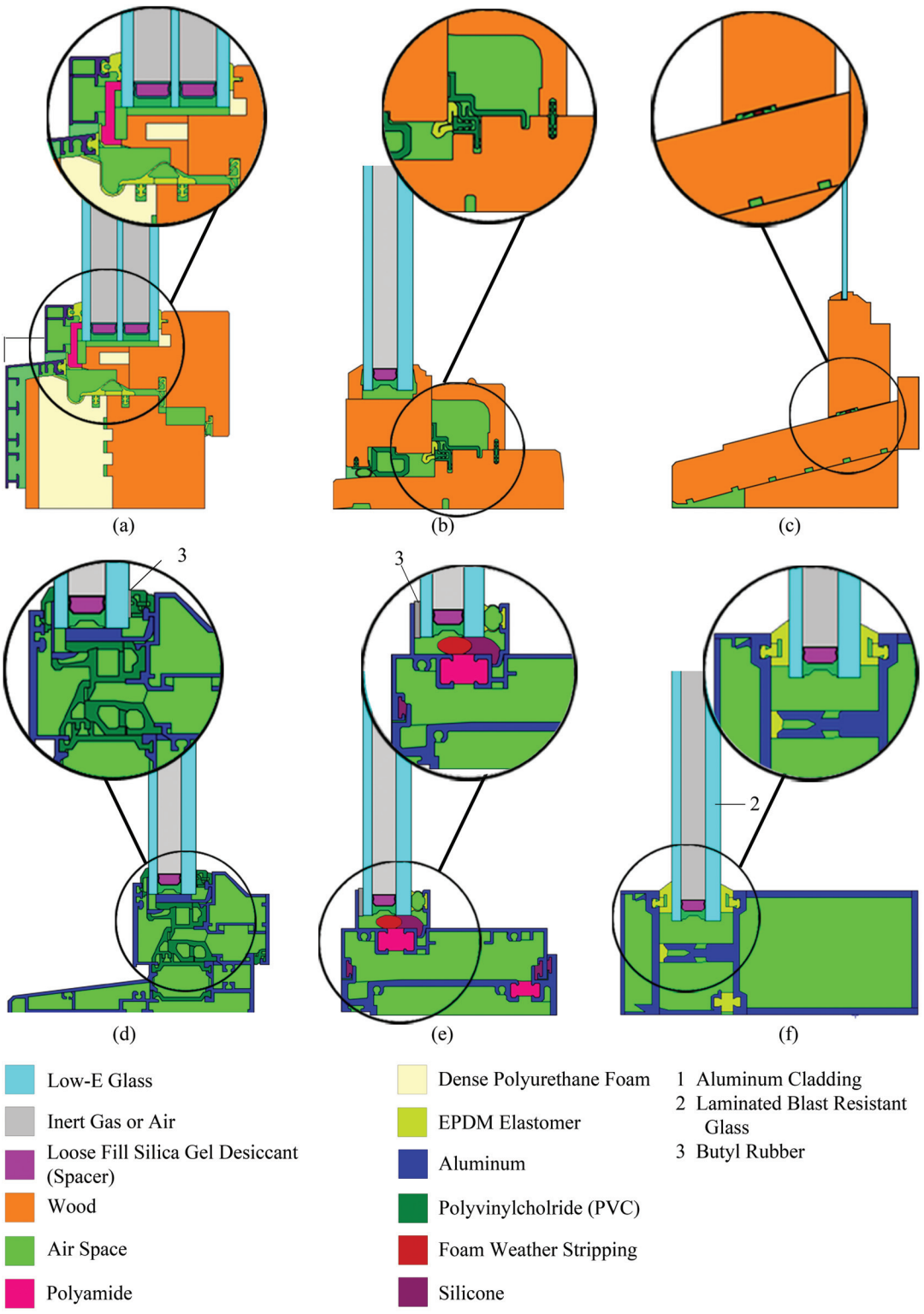

Figure 3 *The six windows examined attempt to capture the range of modern windows, from very high performing triple glazed wood to typical aluminum curtain wall, with progressively lower frame U-factors (note, overall window U-factor does not decrease in the same order, largely due to the single-pane glazing for the low performance wood).*

2. Internal glazing surfaces take their boundary condition from an automatic THERM computation, which uses the center-of-glass temperature computed by WINDOW. Radiation is handled the same as with other internal surfaces.
3. External Surfaces are assigned a convection coefficient of 26 (m^2·K) (4.6 Btu/h·ft^2·°F), which corresponds to a 5.5 m/s (12 mph) wind. Radiation is modeled as communication with a black body at –18°C (–0.40°F) and a view factor of 1. Air temperature is also taken to be –18°C (–0.40°F).
4. Adiabatic surfaces are used on the bottom of windows when they are modeled to determine their component U-values.The glass is extended high enough that it can effectively be cut at an adiabat as well. Walls also extend down far enough that they are terminated at an adiabatic boundary condition. Clear-walls simulations to determine $U_{\text{clear-wall}}$ are also terminated at their top and bottom at an adiabat.

Each of the 24 resulting combinations of wall type, sill detail, and window is then simulated in three different configurations:

1. Baseline thermal bridge: In this case, sill details are in place, but the surfaces where a window frame would touch the wall are given adiabatic boundary conditions. The window itself is not included, but the adiabat must be of the correct depth. Any trim that would block the inside surface of the window is not included, as in Figure 4(a). The thermal coupling coefficient predicted by the simulation is input as L_{2D} in Equation 1, and $U_{\text{window}}h_{\text{window}}$ is input as zero. The Ψ -value solved for is identical for any window of the same depth. It estimates the thermal bridge effect of all masonry sills, additional framing and flashing, but excludes the effect of thermal interaction with the window frame and any effect of trim blocking the inside surface of the window frame.
2. Window installed without trim: In this case, the window is simulated attached to the wall with the appropriate shim gap and sealant and allowed to interact with the wall conductively and, to a limited extent on the interior sill, radiatively. Trim is still not included. See Figure 4(b). The thermal coupling coefficient from the simulation is again used as L_{2D} in Equation 1, but $U_{\text{window}}h_{\text{window}}$ is no longer zero. Any change in the thermal bridge effect from Case 1 is attributed to thermal coupling with the window.
3. Full assembly: In this case, the window is simulated as in Case 2, but realistic interior trim is included, as in Figure 4(c). All trim modeled is 16 mm (5/8 in.) gypsum wall board. Computation of thermal bridge effect is similar to Case 2. Any change in the thermal bridge effect from Case 2 is attributable to the effects of covering part of the interior of the window frame and, to a lesser extent, part of the interior wall.

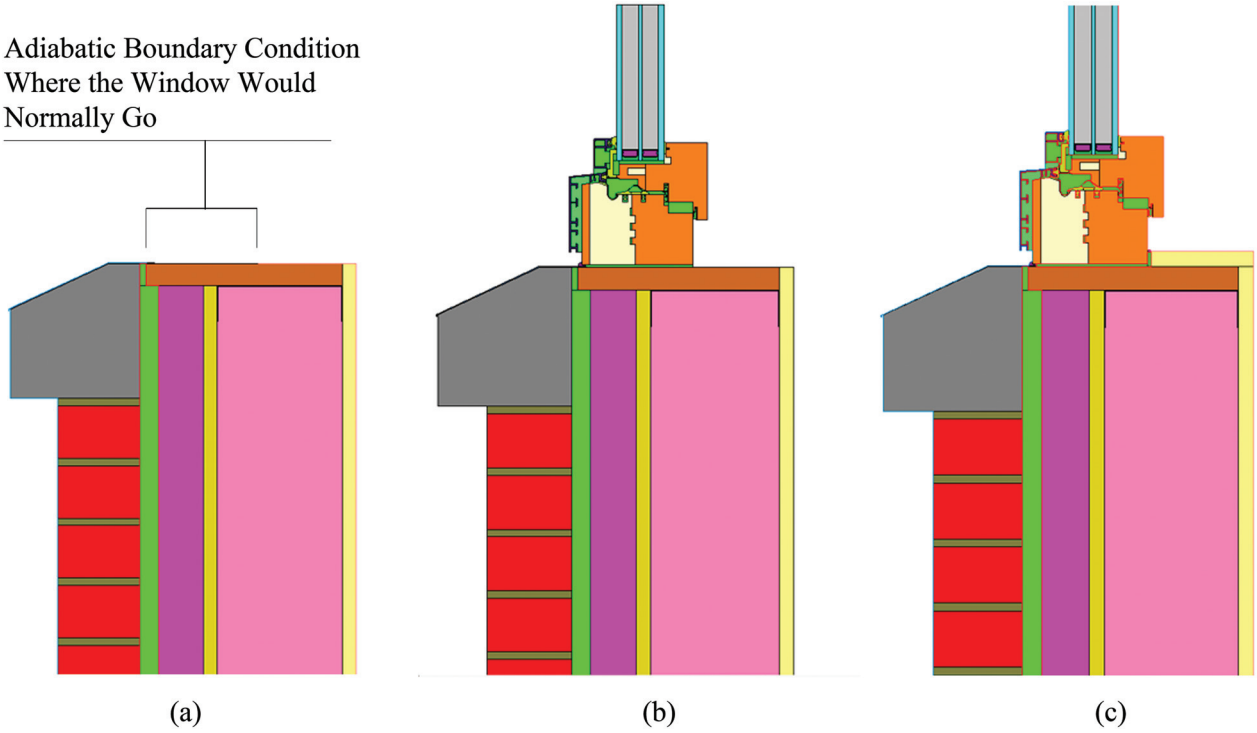

Figure 4 *The different thermal bridge cases including a) the baseline thermal bridge, b) the thermal bridge including window coupling effects, and c) the thermal bridge including the effects of interior trim on the wall and window.*

RESULTS

Tables 1 and 2 show the results from the clear-wall and window simulations, and Table 3 shows the Ψ -values for each window-wall combination for the bridged and unbridged case. Figure 5 displays the primary results in terms of L_{2D} from Equation 1, color coded to match Figure 1. Note that the top bar is a function of the window only, excluding any trim effects, while the bottom bar is a function of the wall only, excluding any sill details. The middle bar encompasses trim effects, masonry sills, additional framing, flashing, and all interactions between the wall and the window. The relationship between this quantity and the window in the assembly is the focus of this study.

Table 1. Clear-Wall U-Factors of the Walls Analyzed

	Description	U-Factor, W/(m²·K) (Btu/h·ft²·°F)
Wall A	8 in. CMU with 2 in. rigid insulation and brick veneer	0.382 (0.0673)
Wall B	6 in. stud, 24 in. o.c. with batt insulation, 2 in. rigid insulation and brick veneer	0.247 (0.0435)

Table 2. Window Properties (Note Progression of Frame U-Factors)

	Description	Center of Glass Height	Edge of Glass Height	Frame Height	Center of Glass U-Factor	Edge of Glass U-Factor	Frame U-Factor	Whole Window U-Factor[1]
		mm (in.)			W/(m²·K) (Btu/h·ft²·°F)			
1	Wood, high performance	86.5 (3.41)	63.5 (2.5)	135 (5.32)	1.08 (0.190)	1.20 (0.211)	0.81 (0.143)	1.00 (0.176)
2	Wood, medium performance	86.5 (3.41)	63.5 (2.5)	73.6 (2.90)	1.93 (0.340)	2.41 (0.424)	1.68 (0.296)	1.96 (0.345)
3	Wood, low performance	86.5 (3.41)	63.5 (2.5)	98.7 (3.89)	6.06 (1.07)	5.93 (1.04)	2.67 (0.470)	5.11 (0.900)
4	Aluminum, high performance	86.5 (3.41)	63.5 (2.5)	76.3 (3.00)	1.91 (0.336)	2.14 (0.377)	4.62 (0.834)	2.53 (0.446)
5	Aluminum, medium performance	86.5 (3.41)	63.5 (2.5)	65.9 (2.59)	1.92 (0.338)	2.31 (0.407)	6.20 (1.09)	2.79 (0.491)
6	Aluminum, low performance	86.5 (3.41)	63.5 (2.5)	68.1 (2.68)	1.87 (0.330)	2.03 (0.358)	8.03 (1.41)	3.09 (0.544)

1. Window U-factors are computed for rough comparison only, assuming a window 1200mm by 1500mm with jamb and head U-factors equivalent to sill U-factors.

Table 3. Resulting Ψ-Values for All Assemblies

		With Bridged Sill Details, W/(m·K) (Btu/h·ft·°F)		With Unbridged Sill Details, W/(m·K) (Btu/h·ft²·°F)	
		CMU Wall	Steel Stud Wall	CMU Wall	Steel Stud Wall
1	Wood, high performance	0.297 (0.172)	0.346 (0.200)	0.0263 (0.0152)	0.0332 (0.0192)
2	Wood, medium Performance	0.306 (0.177)	0.362 (0.209)	0.0256 (0.0148)	0.0359 (0.0207)
3	Wood, low performance	0.258 (0.149)	0.317 (0.183)	0.00756 (0.00437)	0.0192 (0.0111)
4	Aluminum, high performance	0.257 (0.149)	0.324 (0.187)	0.0162 (0.00938)	0.0204 (0.0118)
5	Aluminum, medium performance	0.306 (0.177)	0.347 (0.201)	0.0809 (0.0468)	0.0725 (0.0419)
6	Aluminum, low performance	0.307 (0.177)	0.305 (0.176)	0.0785 (0.0453)	0.0799 (0.0462)

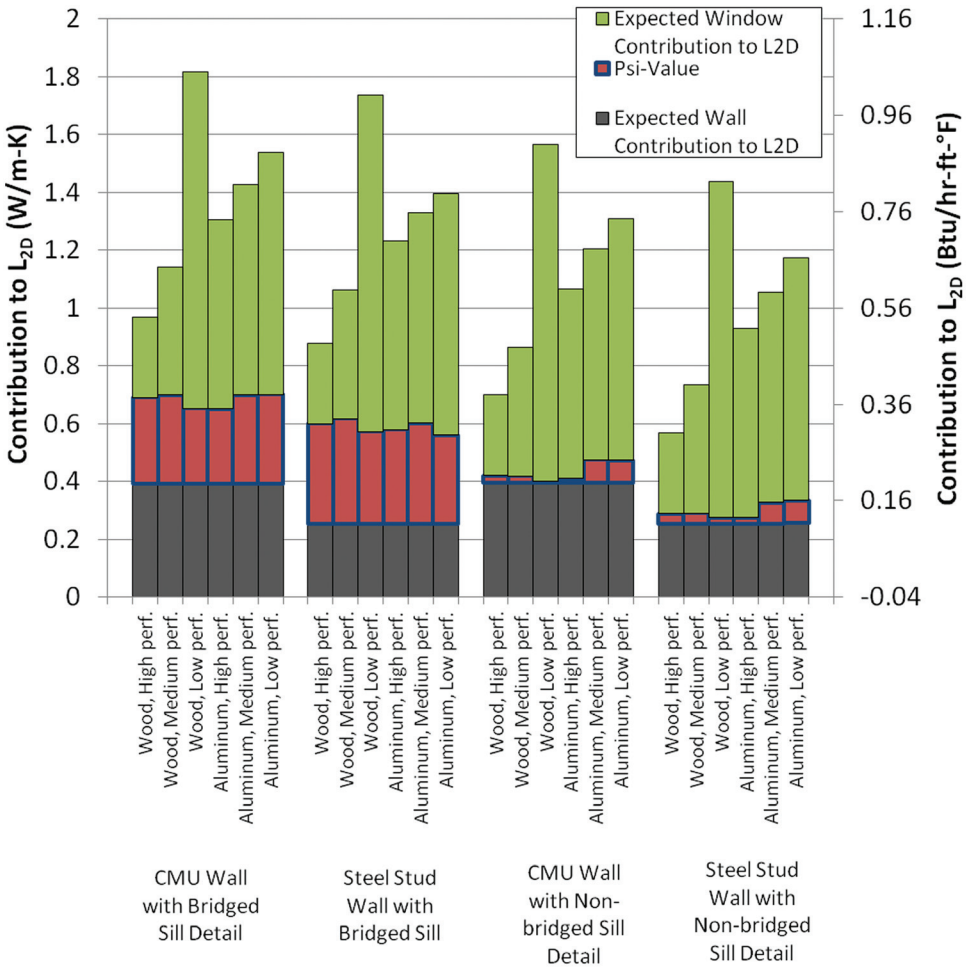

Figure 5 *The thermal coupling coefficient of each assembly. The contributions are separated into those from the wall, the contribution from the window, and the thermal bridge effect. Colors match those of Figure 1. Note that the expected contribution for the wall is based on the height of the wall used in the assemblies and the expected contribution for the window is also for only that height of window included in the assembly (see Table 2).*

Figure 6 shows the thermal bridge effects broken down into components for each of the window-wall combinations for the bridged details. Figure 7 shows it for unbridged details. The window interaction is the change in thermal bridging with the addition of the window. The trim contribution is the reduction in thermal bridging caused by the addition of 16 mm (5/8 in.) interior gypsum trim. This progression is described above and shown in Figure 4.

The window interaction effect can be broken into conduction and radiation effects. If we limit our discussion to conduction heat transfer, it is clear that the insertion of any real window in place of the baseline case will not decrease heat flux. It can only increase thermal cross section—that is, the possible heat transfer paths at every point through the wall. For example, heat transfers from the masonry sill into the highly conductive window frame through most of the depth of the window; at the spacer, the reverse happens, effectively using the masonry to bridge the spacer.

Radiative interaction, however, does not always increase the heat flow. The interior sill surfaces can partially "see" the window frame and glass. In the baseline case, which captures a detail thermally decoupled from the window, all they can see is a 23.0°C (73.4°F) surface, which could tend to cause more room heat to radiatively transfer to the surface without the window.

In some cases, this effect dominates the conductive coupling effect, causing the overall coupling effect to be negative; this is especially true for the low-performance wood window, which gives the interior sill a generous view of cold single pane glass. It is also evident in severely bridged walls, where a substantial bridging element has a large view factor to the window.This example shows that the presence of a window can actually reduce the calculated thermal bridge effect, but this is likely only true in particularly strange cases. The total heat flow, of course, increases over the baseline case with the addition of a window, even with the negative impact to Ψ_{sill};

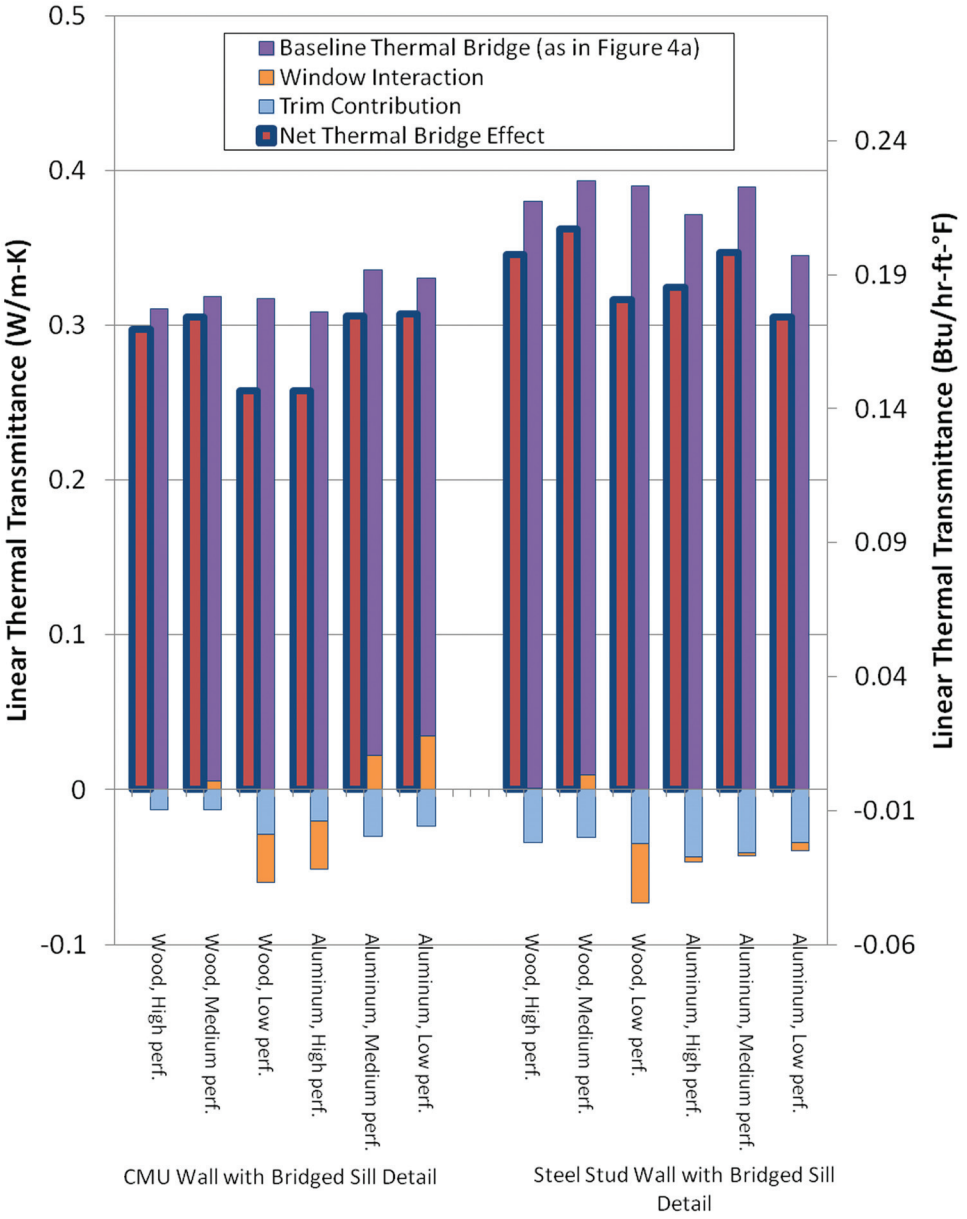

Figure 6 *The net ψ_{sill} from Figure 5 for every window on the bridged details, broken into components determined from the series of simulations described in Figure 4.*

it is obvious from Figure 5 that a poor window cannot make up for its high U-factor with its small reduction in Ψ_{sill}.

Trim, on the other hand, always decreases the calculated Ψ_{sill}. In part, this is attributable to insulating the inside wall beyond the baseline case. The greater contribution, however, is insulating a part of the inside edge of the window frame, which would otherwise exhibit very cold temperatures and substantial heat flux. This latter effect does not occur by any actual thermal bridging reduction, but rather because of an unaccounted for reduction in the heat flow from the interior window frame surface, making the window behave differently than is assumed during the NFRC window simulation and, subsequently, in the application of Equation 1.

The magnitudes of the coupling and trim effects will be discussed separately for the bridged and unbridged cases.

Bridged Details

For all windows on the bridged details, the net thermal bridge effect is severe, mostly owing to the bridging inherent in the details themselves, not window interaction or trim. For the CMU wall, the Ψ_{sill} values are equivalent to adding between 0.67–0.80 m (2.2–2.6 ft) to the clear-wall height. For the steel stud wall, it is 1.3–1.5 m (4.1–4.8 ft). Table 4 shows

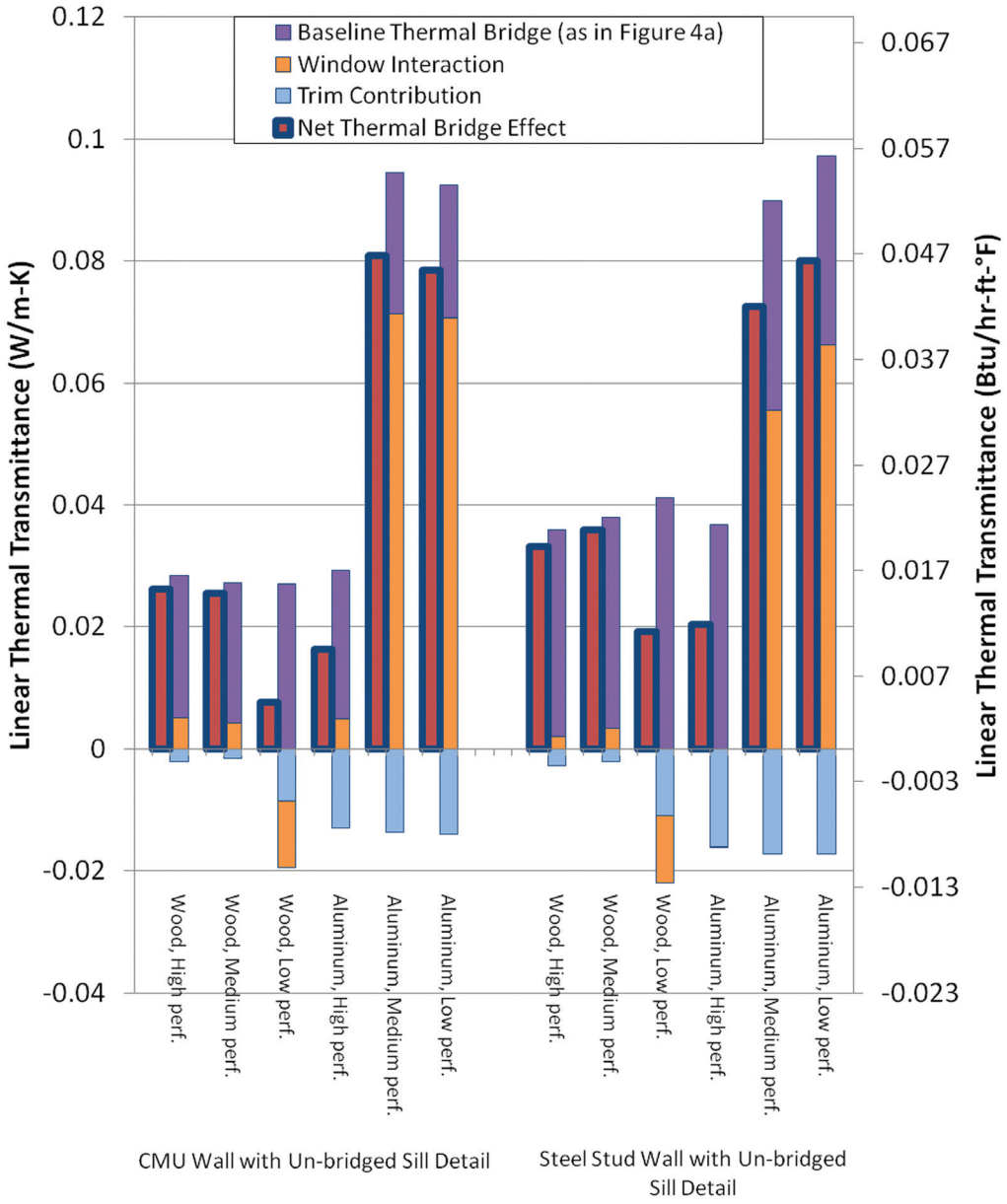

Figure 7 *The net Ψ -value from Figure 5 for every window on the unbridged details, broken into components determined from the series of simulations described in Figure 4.*

Table 4. Statistics for Bridged Details Across All Six Windows

	Average Ψ_{sill}, W/(m·K) (Btu/h·ft·°F)	Standard Deviation of Ψ_{sill}, W/(m·K) (Btu/h·ft·°F)
CMU Wall	0.288 (0.167)	0.0242 (0.0140)
Steel Stud Wall	0.334 (0.193)	0.021 (0.0124)

the average and standard deviation of the Ψ_{sill} for the bridged details across all six windows. The thermal bridge is dominated by the effects of the masonry sills, steel reinforcement, and flashing; trim and window interaction play a minor part. This indicates that a catalog containing these details could purport, with reasonable accuracy, to be relevant for any window installed in the insulation plane. With thermal bridges this severe, temperature gradient through the wall does not encourage heat flow to short-circuit through the window; there is no continuous thermal control layer to short-circuit around.

Unbridged Details

The range in the unbridged CMU wall details of Ψ_{sill} is equivalent to the additional heat flow caused by between 0.02–0.21 m (0.065–0.69 ft) of additional clear wall. For the steel stud wall, the equivalent additional clear wall would be 0.08–0.32 m (0.26–1.1 ft). Table 5 shows the average and standard deviation of the Ψ_{sill} for the unbridged details across all six windows. Though the absolute deviation from the baseline thermal bridge is small, the relative deviation is quite large. This can be substantial if one is attempting to minimize thermal bridges. The baseline Ψ_{sill}'s for the unbridged are on the same order of the Ψ-value cutoff for consideration in the passive house standard, which is 0.01 W/(m·K) (0.006 Btu/h·ft·°F). Below this value, a thermal bridge does not have to be considered during calculations for Passive House certification. For designers attempting this level of performance, deviations seen here can mean a great deal.

The window interaction impact increases the thermal bridge effect in all of the unbridged cases, except for that of the low performance wood window. This is likely due to minimal conductive coupling and strong radiative coupling due to the single pane glass. In all other wood cases, and in the high performance aluminum case, the interaction is small. In the lower performing aluminum windows, however, the interaction dominates the thermal bridge effect. This effect is not seen for the bridged details because they have temperature gradients that do not tend to encourage heat flux through the windows; in the unbridged case, however, a conductive path through a window can short circuit an otherwise well maintained thermal control layer.

CONCLUSIONS

It is important to remember that the primary window-related increase in heat flux over the clear wall is captured in the U-factor of the window chosen, not in the thermal bridge effect. For all but the highest performing window in this study, a mere 250 mm or less of window frame and glass exhibits heat flux greater than over 1 m of clear-wall height and also greater than any thermal bridge effect, even in the badly bridged details (see Figure 5). That is, when one looks at the whole picture, it is obvious that the minor reductions in thermal bridging evident with some windows do not justify choosing that window over with a higher overall U-factor.

For badly bridged details (e.g., those with masonry sills and metal flashing passing through the insulation plane) the window frame choice does not strongly change the Ψ-value of the thermal bridge. The additional thermal cross section provided by allowing the window to interact conductively does not greatly increase heat flux when the existing thermal path is already quite conductive. This means that such details can be presented in a catalog for use with nearly any window.

For details that maintain the thermal control layer, however, different windows in the same sill detail give rise to relatively large Ψ-value differences, especially relative to Ψ-values of details that meet Passive House level performance. In fact, the baseline thermal bridge can be magnified by a factor of up to 3.6 by choosing a poorly performing window. This alone makes it difficult to publish a Ψ-value for a particular detail, since it is really a property of the sill detail in combination with the window frame. The trim effects are also quite large in the unbridged cases for window frames that would otherwise have a very cold inside surface. As such, a catalog entry for high performing details would need caveats limiting its use to situations in which the details are combined with high performance windows.

Table 5. Ψ_{sill} Statistics for Unbridged Details Across All Six Windows

	Average Ψ_{sill}, W/(m·K) (Btu/h·ft·°F)	Standard Deviation of Ψ_{sill}, W/(m·K) (Btu/h·ft·°F)
CMU Wall	0.0392 (0.0226)	0.0321 (0.0186)
Steel Stud Wall	0.0435 (0.0251)	0.0263 (0.00152)

REFERENCES

Cappelletti F., Gasparella A., Romagnoni P., Baggio P. 2011. Analysis of the influence of installation thermal bridges on windows performance: The case of clay block walls. 2011. University IUAV of Venezia, Venezia, Italy

Finlayson, E., Mitchell R., Arasteh D., Huizenga C. and Curcija D. 1998. THERM 2.0: Program description. A PC program for analyzing the two-dimensional heat transfer through building products. University of California, Berkeley, CA, USA.

International Organization for Standardization (ISO). ISO 10211. 2007. *Thermal bridges in building construction –Heat flows and surface temperatures– Detailed calculations*. Geneva, Switzerland: ISO.

International Organization for Standardization (ISO). ISO 14683. 2007. *Thermal bridges in building construction –Linear thermal transmittance – Simplified methods and default values*. Geneva, Switzerland: ISO.

International Organization for Standardization (ISO). ISO 6946. 2007. *Building Components and building elements –Thermal resistance and thermal transmittance– Calculation method*. Geneva, Switzerland: ISO.

Lstiburek, Joseph. 2011. BSI-062 Thermal Bridges Redux. http://www.buildingscience.com/documents/insights/bsi062-thermal-bridges-redux.

Mitchell R., Kohler C., Arasteh D., Huizenga C., Yu T., and Curcija D. 2001. *WINDOW 5.0 User Manual*. Lawrence Berkeley National Laboratory, Berkeley, CA, USA.

Morrison Hershfield. 2011. Thermal Performance of Building Envelope Details for Mid- and High-Rise Buildings (1365-RP). Vancouver, BC, Canada

National Fenestration Rating Council (NFRC). 2010. NFRC 100: *Procedure for determining fenestration product U-factors*. Silver Spring, MD: NFRC.

O'Leary, Thomás. 2012. Thermal Bridge Analysis and Design. High Performance Building Envelope Workshop, March 6–8, 2012, San Antonio, TX, USA.

Schild, Peter G., and Peter Blom. 2010. Good practice guidance on thermal bridges & construction details, Part I: Principles. EPBD, http://buildup.eu/system/files/content/P188_Thermal_bridge_guidance_principles_ASIEPI-WP4.pdf.